

A VGA Optical Filter-less CMOS Image Sensor with UV-selective and Visible Light Channels by Differential Spectral Response Pixels

Yhang Ricardo Sipauba Carvalho da Silva, Rihito Kuroda, and Shigetoshi Sugawa
 Graduate School of Engineering, Tohoku University,
 6-6-11-811, Aza-Aoba, Aramaki, Aoba-ku, Sendai, Miyagi, Japan 980-8579
 TEL: +81-22-795-4833, FAX: +81-22-795-4834, Email address: yhang@dc.tohoku.ac.jp

ABSTRACT

This paper presents a newly developed CMOS image sensor (CIS) capable of capturing UV-selective and visible light images simultaneously in a single exposure, without employing band-pass filters. The developed CIS pixels are composed of high UV sensitivity and low UV sensitivity pixels, arranged alternately in a checker pattern. The UV-selective image is captured by extracting the differential spectral response between adjacent pixels, while the visible light image is captured by the low UV sensitivity pixels. The lateral overflow capacitor (LOFIC) [1] technology was introduced in both pixel types to achieve high sensitivity and wide dynamic range simultaneously. The developed CIS exhibits $172\mu\text{V}/e^-$ conversion gain, $131ke^-$ full well capacity (FWC) and 92.3dB dynamic range. The spectral sensitivity ranges of high and low UV sensitivity pixels are 200-700nm and 370-700nm, respectively, and that of after the differential spectral response extraction is 200-480nm. A UV-selective sample image captured using the developed CIS is presented.

INTRODUCTION

Ultraviolet (UV) imaging is useful for detecting harmful chemical substances [2], flame detection [3], control of semiconductor processes [4] and so on. Obtaining UV light and visible light images simultaneously with a simple optical structure is advantageous for various sensing applications under background visible light.

Several approaches for UV imaging have been reported so far, usually by combining an UV-sensitive image sensor with

optical methods for UV-selective detection. Examples of UV-sensitive image sensors include a CIS with a thin, high concentration and steep dopant profile surface layer in the pixel photodiodes [5-6], a superlattice-doped CCD [7], a BSI CIS with high UV and visible light sensitivity [8], a CIS using UV-sensitive organic photoconductive films [9]. Methods for UV-selective imaging employ on-chip [7] or off-chip [10-11] bandpass filters (BPF), time-shared illumination [12], or image subtraction under constant background light ambient [9] and so on.

In this work, we aimed at developing a CIS capable of simultaneously capturing UV and visible light images in a single exposure, for applications that require UV imaging under variable background visible light. Also, capturing both UV and light spectrum simultaneously has a potential advantage of using the visible light image for region selection, to improving accuracy of the UV imaging.

Previously, we developed a differential spectral response technology for single photodiode (PD) optical sensor [10]. In this work, we developed an optical filter-less CIS outputting UV-selective and visible light images simultaneously in a single exposure, by using differential spectral response pixels. Fig.1 shows the conceptual diagram of the differential spectral response method used in this work [10]. We have developed pixels with high and low UV light sensitivity, with matching sensitivities for visible and NIR light, and arranged both types in the CIS pixel area. With this approach, the UV-selective image is obtained by extracting the differential spectral response of both pixel types, while the visible light image is captured simultaneously by the lowly

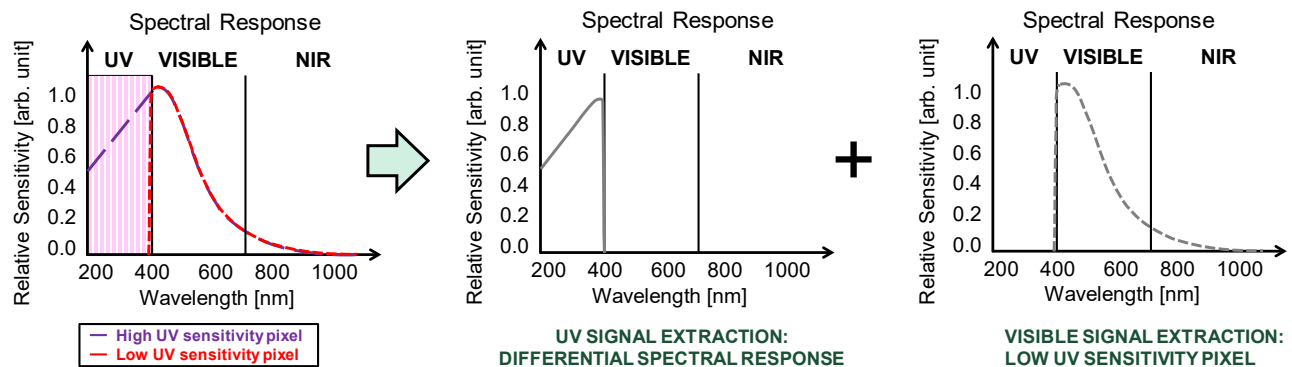


Fig. 1. Conceptual diagram of the developed CIS using differential spectral response pixels. High and low UV sensitivity pixels are implemented in the CIS, and UV light images are extracted from the differential response between both types of pixel. Simultaneously, visible light images are captured by the low UV sensitivity pixels.

UV sensitive pixels. With our approach, band-pass filters such as on-chip or external optical filters are not necessary, and UV-selective and visible light images can be captured by a single image sensor. The lateral overflow integration capacitor (LOFIC) [1] technology was introduced, to achieve high sensitivity and wide dynamic range simultaneously.

As an example of UV and visible light simultaneous imaging, we captured images of male and female cabbage butterflies illuminated by UV and visible light, aiming at sex identification by analyzing the light absorption characteristics in the UV and visible wavebands.

DESIGN AND STRUCTURE OF DEVELOPED CMOS IMAGE SENSOR

We developed new pinned PD structures for the high and low UV sensitivity pixels employed in the CIS of this work. By leveraging the relationship between light wavelength and penetration depth in Si, we determined the PD structures to obtain high and low UV sensitivity, without changing sensitivity for the visible and NIR wavebands. This approach is possible because the penetration depth of light in Si generally increases with the wavelength, from a few to thousands of nanometers in the 200-1100nm range. By adjusting the internal doping conditions and creating potential barriers in the PD structure, it is possible to control the spectral sensitivity.

Fig. 2 shows the cross-sectional structure of each type of pixel, and their respective internal potential diagrams. The high UV sensitivity pixel PD (PD1) has a similar structure near Si surface to a previously mentioned PD with high 190-1100nm sensitivity [5-6]. However, a p-well layer was introduced to reduce visible and NIR light sensitivity by forming a potential barrier at depth of approximately 480nm from the Si surface. The low UV sensitivity pixel PD (PD2) has a surface N⁺ layer added to form a potential barrier at 20-40nm from the Si surface, to reduce UV light sensitivity. The

same p-well layer employed in PD1 was used to match sensitivity for visible and NIR light between the photodiodes. In PD2, photo-electrons generated near the Si surface by UV light are drifted by the internal potential to the surface N⁺ layer and undergo recombination or are drained out, selectively extinguishing UV sensitivity.

In the pixel PD design, the internal potential barriers depth necessary for each type of photodiode were determined by calculating an estimative of the internal quantum efficiency (QE_{int}), according to the following equation.

$$QE_{int}(\lambda) = e^{-\alpha*d1} - e^{-\alpha*d2} \quad (1)$$

Here, α is the absorption coefficient of Si for the wavelength λ , and d1 and d2 are the depths of the potential barriers due to the surface layers (d1) and the p-well layer (d2), respectively. In the derivation of Eq. 1, we assumed that all photo-electrons generated between the potential barriers d1 and d2 are detected, and that none of the photo-electrons generated outside this region are detected.

For PD1, the depth d1 was set in order to obtain QE_{int} of 100% in the UV light waveband. For PD2, it was set to obtain QE_{int} of lower than 10% for wavebands shorter than 370nm. Similarly, d2 was set to obtain QE_{int} lower than 10% for wavelengths longer than 700nm in both pixel types. From the calculations, we determined that d1 and d2 should be of 0nm and 480nm for PD1, and 30nm and 480nm for PD2, respectively. Doping condition for the surface N⁺, surface P⁺, buried N and p-well layers were determined to meet those requirements.

The circuit architecture and pixel array arrangement are shown in Fig. 3. High and low UV sensitivity pixels were arranged alternately, in a checker pattern, to facilitate the differential signal extraction. In order to achieve high sensitivity and wide dynamic range simultaneously, LOFIC [1] technology was introduced.

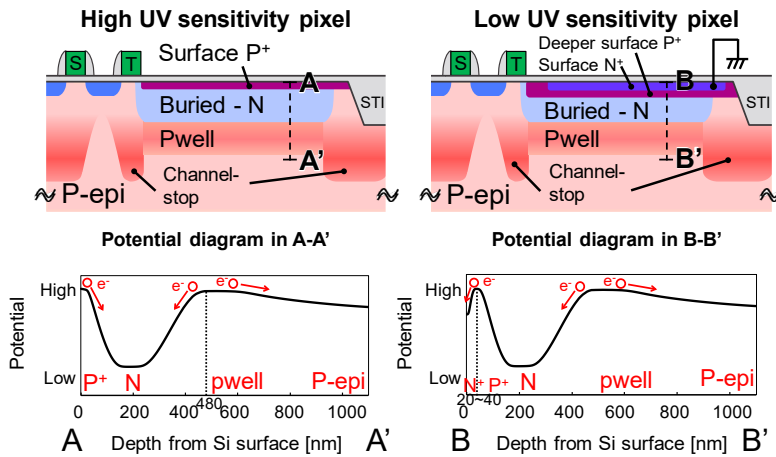


Fig. 2. Cross sectional structure and simulated potential diagrams of the photodiodes employed in the high UV sensitivity pixel (left) and the low UV sensitivity pixel (right).

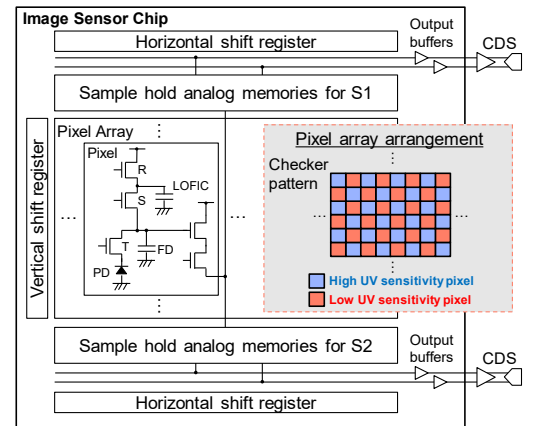


Fig. 3. Circuit architecture and pixel array arrangement. Pixels were arranged in a checker pattern to facilitate the differential signal extraction. LOFIC was implemented.

CHIP FABRICATION AND MEASUREMENT RESULTS

Using the developed pixel structures, a CIS was fabricated with a $0.18\mu\text{m}$ 1-poly-Si 5-metal CIS technology and buried pinned PD. The power supply voltage is 3.3V , the chip die size is $4.8\text{mm}^{\text{H}} \times 4.8\text{mm}^{\text{V}}$, pixel pitch is $5.6\mu\text{m}$, total number of pixels is $648^{\text{H}} \times 488^{\text{V}}$ with $640^{\text{H}} \times 480^{\text{V}}$ effective. The fabricated chip micrograph is shown in Fig. 4.

Fig. 5 shows the measured photoelectric conversion characteristic of the high UV sensitivity pixel, for both the high conversion gain signal S1 and the high saturation signal S2. S1 uses only FD for the photo-electrons to voltage conversion, while S2 uses FD + LOFIC. The conversion gain of S1 was $172\mu\text{v}/e^-$. By combining the high sensitivity and high saturation signals, 92.3dB dynamic range was obtained. The low UV sensitivity pixels showed similar characteristics. Fig. 6 shows the measured spectral sensitivity for the high and low UV sensitivity pixels in terms of external quantum efficiency (QE). The measurement was carried out in 2nm steps, in the range of 200-1000nm with a monochromator with 2nm resolution. From the results, the spectral sensitivity range of the high and low UV sensitivity pixels were of 200-700nm and 370-700nm, respectively. The differential spectral response between the high and low UV sensitivity pixels is shown in Fig. 7. By extracting the differential spectral response, selective sensitivity in the waveband of 200-480nm was obtained, therefore suitable for UV imaging. Table 1 summarizes the performances of the developed CIS.

As an example of UV and visible light imaging, the developed CIS was used to capture images of male and female white cabbage butterflies, with the experimental setup shown in Fig. 8. The butterflies were illuminated by the 20W UV lamp EFD23-SSBK and white LED light source PFBR-150SW-MN, manufactured by Jefcom and CCC Inc., respectively. Images were captured using a 6mm lens, in a single exposure and without employing bandpass filters. The captured images are shown in Fig. 9. In this figure, (a) shows the output from high UV sensitivity pixels, (b) shows the captured visible light image from the low UV sensitivity pixels and (c) shows the UV selective image obtained by the differential spectral response. A simple interpolation consisting of averaging the adjacent pixels was carried out, and a gamma of 2.2 was applied to the images. Both male and female white cabbage butterflies reflect visible light, but only the male absorbs UV light. This feature was successfully captured by the developed CIS.

CONCLUSION

A $640^{\text{H}} \times 480^{\text{V}}$ CIS with high and low UV light sensitivity pixels exhibiting UV-selective and visible light image capturing capability by differential spectral response is presented. The developed CIS successfully captured UV and visible images by a single exposure without optical filters. The developed CIS requires only a few additional ion implantation process steps and is promising for various sensing applications that require UV light imaging under strong or variable background visible light, such as flame detection, food freshness inspection and so on.

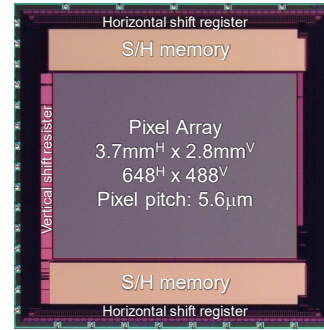


Fig. 4. Developed CIS chip micrograph.

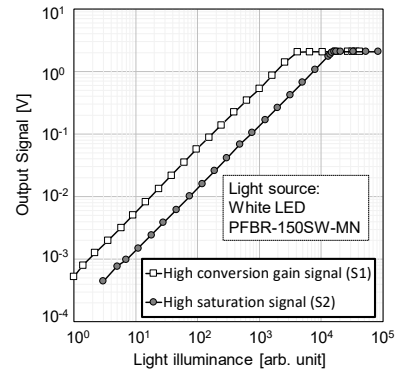


Fig. 5. Photoelectric conversion characteristic.

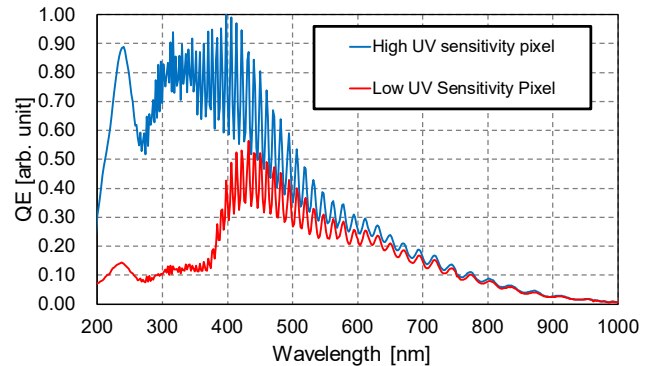


Fig. 6. Measured spectral sensitivity response for the pixels with high and low UV sensitivity.

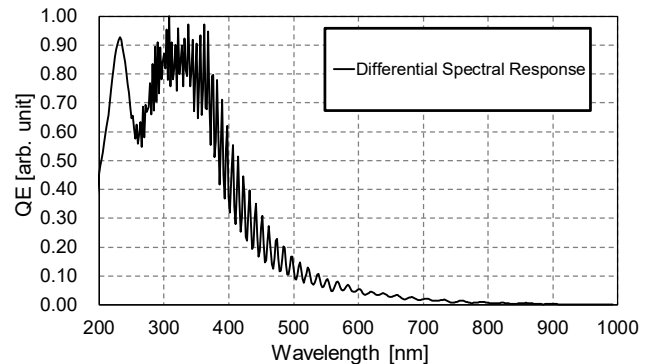


Fig. 7. Differential spectral response. A high selectivity to UV waveband without bandpass filters was successfully achieved.

Table I. Performance summary of the developed CIS.

Process technology	0.18 μm 1P5M CMOS with pinned PD	
Power supply voltage	3.3V	
Die size	4.8mm ^H x 4.8mm ^V	
Pixel size	5.6 μm ^H x 5.6 μm ^V	
Number of pixels	Total	648 ^H x 488 ^V
	Effective	640 ^H x 480 ^V
Aperture ratio	36%	
Frame rate	30fps	
Conversion Gain	172 $\mu\text{V}/e^-$ (S1 signal)	
Full well capacity	131ke ⁻ (S2 signal)	
Dynamic Range	92.3dB	
Spectral sensitivity range	High UV sensitivity pixel	200 – 700nm
	Low UV sensitivity pixel	370 – 700nm
	Differential response	200 – 480nm

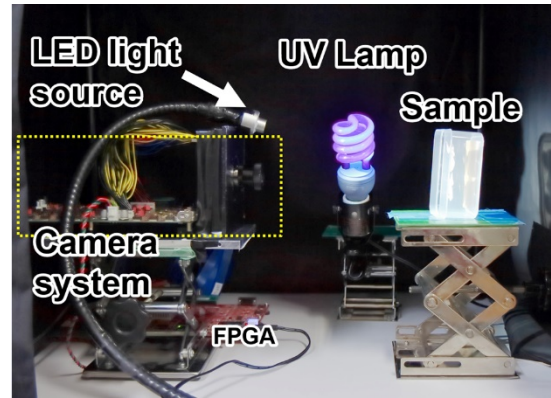


Fig.8. Setup used for capturing sample images of the developed CIS.

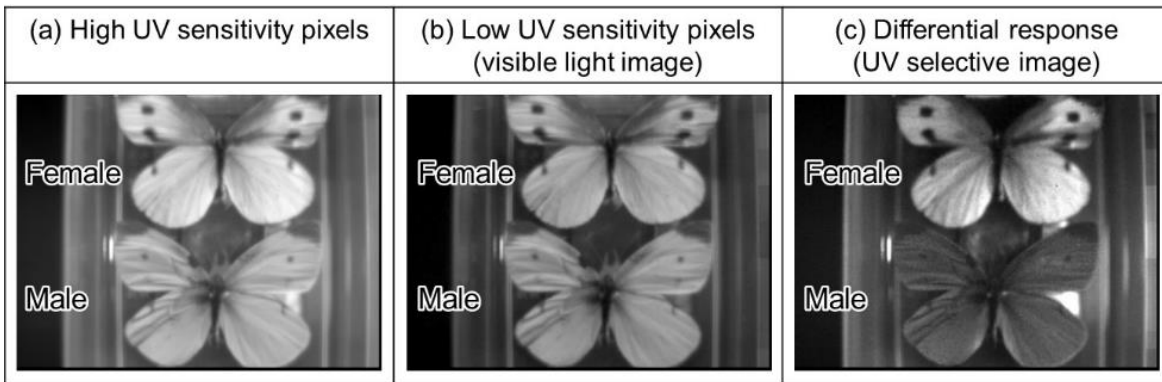


Fig.9. Cabbage white butterflies (top: female, bottom: male) images captured by the developed CIS. (a) shows the output from high UV sensitivity pixels, (b) shows the captured visible light image from low UV sensitivity pixels, and (c) shows the UV selective image obtained by the differential response extraction. All images were captured simultaneously in a single exposure.

REFERENCES

- [1] S. Sugawa, et al., "A 100dB dynamic range CMOS image sensor using a lateral overflow integration capacitor," ISSCC, Digest Tech, pp. 352-353, 603, 2005.
- [2] E. Dupuit, A. Dandrieux, P. Kvapil, J. Ollivier, et al., "UV spectrophotometry for monitoring toxic gases," Analusis 28, pp. 966-972, 2000.
- [3] Z. Djuric, et al., "Silicon resonant cavity enhanced UV flame detector," 23rd International Conference on Microelectronics, vol. 1, pp. 239-242, 2002.
- [4] H. Ishii, M. Nagase, et al., "A high sensitivity compact gas concentration sensor using UV light and charge amplifier circuit," 2016 IEEE SENSORS, pp. 1-3, 2016.
- [5] R. Kuroda, et al., "A Highly Ultraviolet Light Sensitive and Highly Robust Image Sensor Technology Based on Flattened Si Surface," ITE Transactions on Media Technology and Applications, Vol.2, No.2, pp. 123-130, 2014.
- [6] T. Nakazawa, et al., "Photodiode dopant structure with atomically flat Si surface for high-sensitivity and stability to UV light," SPIE-IS&T, Vol.8298, pp. 82980M-1-8, 2012.
- [7] S. Nikzad, et al., "UV/Optical Photon Counting and Large Format Imaging Detectors from CubeSats, SmallSats to Large Aperture Space Telescopes & Imaging Spectrometers," IISW, pp. 352-355, 2017.
- [8] X. Wang, et al., "A 4M, 1.4e⁻ noise, 96dB dynamic range, back-side illuminated CMOS image sensor," IISW, 2015.
- [9] T. Okino, et al., "A Real-Time Ultraviolet Radiation Imaging System Using an Organic Photoconductive Image Sensor," Sensors 18, no. 1:314, 2018.
- [10] N. Gat, "Imaging spectroscopy using tunable filters: a review," Proc. SPIE, Vol.4056, pp. 50-64, 2000.
- [11] Y. Fujihara, et al., "A Multi Spectral Imaging System with a 71dB SNR 190-1100 nm CMOS Image Sensor and an Electrically Tunable Multi Bandpass Filter," ITE, 2018.
- [12] Y. Fujihara, S. Nasuno, S. Wakashima, et al., "190-1100 nm Waveband multispectral imaging system using high light resistance wide dynamic range CMOS image sensor," IEEE SENSORS, pp. 283-285, 2016.
- [13] Y. R. Sipauba Carvalho da Silva, Y. Koda, S. Nasuno, R. Kuroda and S. Sugawa, "An ultraviolet radiation sensor using differential spectral response of silicon photodiodes", IEEE SENSORS, pp. 1847-1850, 2015.